Characterization of newly established clear cell adenocarcinoma cell line (YDOV-21) including comparative genomic and proteomic investigation.

Yong Hyun Chae

Department of Medicine
The Graduate School, Yonsei University

Characterization of newly established clear cell adenocarcinoma cell line (YDOV-21) including comparative genomic and proteomic investigation.

Yong Hyun Chae

Department of Medicine
The Graduate School, Yonsei University

Characterization of newly established clear cell adenocarcinoma cell line (YDOV-21) including comparative genomic and proteomic investigation.

Directed by Professor Jae-Hoon Kim

The Master's Thesis
submitted to the Department of Medicine
the Graduate School of Yonsei University
in partial fulfillment of the requirements for the degree of Master of Medical Science

Yong Hyun Chae

June 2010

This certifies that the Master's Thesis
of Yong Hyun Chae is approved.

Thesis Supervisor : Jae-Hoon Kim

[Dong Sup Yoon: Thesis Committee Member#1)

[Yun Chae-Ok: Thesis Committee Member#2)

The Graduate School
Yonsei University

June 2010

ACKNOWLEDGEMENTS

This work is partially supported by scholarship of The Graduate School, Yonsei University. I really appreciate Professor Jae-Hoon Kim for his great advice on this work and thank Yoon Jin Oh and Sun Mi Choi for expert technical assistance. The authors also thank two co-reviewers, Dong Sup Yoon and Yun Chae-Ok for important comments and suggestions on a draft of this paper. Finally, I dedicate this thesis to my wife.

<TABLE OF CONTENTS>

LIST OF FIGURES

LIST OF TABLES

<ABSTRACT>

Characterization of newly established clear cell adenocarcinoma cell line (YDOV-21) including comparative genomic and proteomic investigation.

Yong Hyun Chae

Department of Medicine

The Graduate School, Yonsei University

(Directed by Professor Jae-Hoon Kim)

The establishment of an ovarian clear cell adenocarcinoma (CCA) cell line can facilitate the research for biologic properties of CCA and molecular mechanisms involving carcinogenesis. A new CCA cell line, named YDOV-21, was established from ovarian tissues of a 53-year-old Korean woman diagnosed with FIGO stage IIIb ovarian cancer. It has been maintained in long-term culture. For characterization of YDOV-21, *In vitro* morphology, Growth kinetics, Chemosensitivity test and Tumorigenicity were investigated. To understand the reason of the distinctive clinical features of CCA, comparative genomic profiles and proteomes of the YDOV-21 were also studied. Cultured YDOV-21 showed oval, round or polygonal cells in a pavement-like arrangement, piled up without contact inhibition. The cultured cells were easily adherent dish bottom and spread as a sheet of monolayer cell. Doubling time of YDOV-21 showed 28.7 hours. Chemosensitivity test revealed that the most sensitive chemotherapeutic agent was gemcitabine among the twelve tested drugs. YDOV-21 had a high tumorigenic potency in nude mice. The cell line showed rapid growth kinetic and early metastasic capacity. cDNA Microarray test revealed that 3,983 genes were up-regulated and 4,188 genes were down-regulated in the YDOV-21 cell line in comparison to four HOSEs (> five-fold, $P < 0.05$). Selected up-regulated genes were validated with SYBR Green real-time RT-PCR. Protein profiles were identified by 2-DE and MALDI-TOF/PMF method. In this analysis, 31 up-regulated spots were observed at least two-fold difference in the YDOV-21 than HOSEs as a control cell. The result of this study can be a valuable resource for the CCA investigation.

Key words: Cell line, Clear cell adenocarcinoma, Microarray, proteomic profile, 2D

Characterization of newly established clear cell adenocarcinoma cell line (YDOV-21) including comparative genomic and proteomic investigation.

Yong Hyun Chae

Department of Medicine

The Graduate School, Yonsei University

(Directed by Professor Jae-Hoon Kim)

I. Introduction

Although comprising 3-12.1% of all the ovarian cancers, the clear cell adenocarcinma(CCA) has received attention due to the controversy in their histopathological classifications, poor prognosis, and distinctive clinical characteristics [1]. CCA is well-known for its distinctive clinical features as follows : 1) CCA often associated with endometriosis; 2) most patients are International Federation of Gynecology and Obstetrics (FIGO) Stages I or II when the CCA was diagnosed; 3) CCA is more resistant to systemic chemotherapy than other ovarian adenocarcinoma; 4) although opinions differ as to the prognosis, some have reported a worse prognosis than other type of ovarian carcinoma; 5) it often is accompanied by a thromboembolic complication; and 6) hypercalcemia is observed at a high frequency [2]. Although many investigations on CCA have been performed, long-term prognosis for patients with advanced disease has not improved significantly. It was thought that mainly because no effective treatment strategies were existed.

Genetic alteration is the major cause of carcinogenesis. So, the development of new strategies for diagnosis and treatment must be based on a cellular biology. In order to investigate the cellular biology of the malignancy, it is very important to have clinically relevant *in vitro* models to help us. Although several CCA cell lines have been established, no single cell line holds all information of cancer cell properties. So, establishing a novel cell line and its characterization can serve as valuable resource for CCA investigation. For all this, there are relatively small numbers of CCA cell line have been introduced than other type of ovarian malignancy.

In the current study, to understand the reason of the distinctive clinical features of CCA, molecular mechanisms have been investigated. However, the abnormalities of one or a few molecules that have been detected by traditional methods are insufficient to explain the characteristics of CCA [3]. In this problem, comprehensive genetic analysis of YDOV-21 using cDNA microarray was performed. After then the result was validated with SYBR Green real-time RT-PCR method.

Protein molecule is functional effecter of the gene. So studying profiles of protein expression can lead to biologic insights and potential improvements in diagnosis and treatment of CCA. By means of proteomic analysis with two-dimensional electrophoresis (2-DE), followed by matrix-assisted laser desorption ionization time of flight and protein mass fingerprinting (MALDI-TOF/ PMF) and database searching, we could examine the profiles of YDOV-21 and serve basis to CCA proteome research.

In this study, we successfully established a novel CCA cell line named YDOV-21 and characterized its properties including general characteristics (*In vitro* morphology, Growth kinetics, Chemosensitivity test), Tumorigenicity and genomic / proteomic profiles.

II. Materials and methods

1. Origin of the cell line

This cell line was established in November, 2005 from ovarian tissues of a 53-year-old Korean woman diagnosed with FIGO stage IIIb ovarian cancer. The patient underwent total hysterectomy and both adnexectomy. The pathologic diagnosis was clear cell carcinoma. The patient received 6 courses of chemotherapy with Carboplatin and Paclitaxel.

When Carcinomatosis was developed in 2006, the patient was treated with 6 additional courses of chemotherapy with Carboplatin and Etoposide. Due to aggravated carcinomatosis, the patient was expired on 2007.

2. Primary culture and culture conditions

During operative procedures, a tumor specimen was trimmed of adipose and necrotic tissue under aseptic conditions and was washed more than 3 times with phosphate-buffered saline (PBS). The specimen were minced with scissors (to 1-2mm^3 blocks) in Medium 199 (Gibco, Grand island, NY) and MCDB 105 (1:1) (Sigma, St Louis, Mo) supplemented with 15% fetal bovine serum (FBS) (Gibco, Grand island, NY), 2 mM sodium bicarbonate, penicillin 100 IU/ml, and streptomycin 100 μg/ml. After washings, the cells were seeded into 60 mm^2 culture dish. All cultures were maintained at 37°C in a humidified 5% CO_2 ambient air atmosphere. When these outgrowth cultures formed confluent monolayer, the cells were washed twice with PBS and subcultured in 0.25 % trypsin with 1mM ethylenediaminetetraacetic acid(EDTA).

3. Mycoplasma contamination test

We performed a test to confirm possible contamination with mycoplasma by using of polymerase chain reaction (PCR)-based method in the newly derived cell lines according to the manufacturer's instructions (*i*-MycoPCR mycoplasma detection kit; iNtRON Biotechnology Inc., Seongnam, Korea).

4. *In vitro* morphology

To examine the morphology of the cell lines, Cultured cells were observed daily with phase-contrast microscopy (Olympus, Tokyo, Japan) and were histopathologically compared with the Induced cell. For transmission electron microscopic study, the obtained specimen was prefixed with 3% PBS 4℃ for 1 hour and was postfixed with 1% phosphate-buffered osminum tetroxide, it was washed with alcohol and substituted with propylene oxide followed by embedding process in Epon mixture. the specimen was sliced into ultra-thin section and double-stained with Uranyl acetate and

lead citrate. Then we examined the specimen with transmission electron microscope (TEM; Philips Scientifics, Eindhoven, The Netherlands).

5. Growth kinetics

We analyzed the growth curve and population doubling time to understand the growth characteristics of the cell line. We analyzed the growth curve using Cell Titer 96® Aqueous one Solution cell proliferation Assay (Promega, Madison, WI). We seeded $3x10^3$ cells in 96 well plates with 100 μl culture media. Without and with 10%, 15% FBS, we analyzed the growth pattern every other day during 6 days. We added 20 μl of MTS (a novel tetrazolium compound [3-(4,5-dimethylthiazol-2-yl)-5-(3-carboxymethoxyphenyl)-2-(4-sulfophenyl)-2H-tetrazolium, inner salt; MTS[(a)]]) solution in every well of 96 well plates and cultured the cells for four hours in a 37 ℃ incubator, then measured the optical density (OD) value at 490nm using ELISA reader (EL311, Bio-tek Instruments, NY, USA). Thus, we found out cell growth kinetics from the growth curve. The assay was performed 3 times.

6. Chemosensitivity test

For chemosensitivity test, we employed Adenosine triphosphate-based chemotherapy response. Briefly described, the cells were seeded in 96-well plates. Three days after plating, we pretested each anticancer drug on untreated control and treated group to determine PPC (Peak Plasma Concentration). The anticancer drugs used were gemcitabine, etoposide, 5-fluorouracil, doxetaxel, doxorubicin, irinotecan, paclitaxel, oxaliplatin, cisplatin, bleomycin, carboplatin, and tototecan. Each test was carried out at the drug concentration 0.2X, 1X, 5X of PPC. Cells from the untreated control and treated group were lysed, and the amount of ATP in the cell lysates measured using luciferin and excessive luciferase (Roches, Mannhein, Germany), followed by flash type luminescence measurements on a Victor 3 multi-label counter (PerkinElmer, Boston, MA). We calculated the Chemosensitivity index (CI) as follows: 300 – SUM (% cell suppression 0.2 X − 5 X).

7. Tumorigenicity

Tumor-forming ability was tested by inoculating $2 X 10^3$ cells subcutaneously into 5–week-old nude mice (BALB/c nu/nu, female, Orient Bio, Korea). five nude mice were assigned. We measured the size of tumor mass every two days. The mice were sacrificed on the 56^{th} day. Induced tumor mass, liver, lung, kidney, ovary, heart, omentum, stomach, spleen and visible metastatic mass were fixed and processed routinely to obtain paraffin sections. Stained with hematoxylin and eosin (H&E), the specimens were compared with the original slides.

8. cDNA microarray

Total RNA of YDOV-21 and four human ovarian surface epithelial cells (HOSEs) (HOSE 198, 209, 211,213) were isolated by using RNeasy Mini Kit (Qiagen, Valencia, CA). After then the total RNA was purified using RNeasy columns (Qiagen, Valencia, CA) according to the manufacturer's protocol. Ambion Illumina RNA amplification kit was applied to get biotinylated cRNA in the accordance with the manufacturer's instructions (Ambion, Austin, TX). After this, by using a ND-1000 Spectrophotometer (NanoDrop, Wilmington, DE), the cRNA was quantified. A total of 750 ng of labeled cRNA samples were hybridized to each Sentrix Human Ref-6-V2 Expression Bead Chip according to the manufacturer's instructions (Illumina Inc., San Diego, CA). Detection of array signals was executed by using Amersham fluorolink streptavidin-Cy3 (GE Healthcare Bio-Sciences, Little Chalfont, UK) according to the Bead Chip protocol. Arrays were scanned with an Illumina Bead Array Reader according to the manufacturer's instructions. Illumina Bead Studio software was applied to processing and analysis of array data. A total of 25,234 probes were applied in the final analysis. Data were extracted using the software provided by the manufacturer (Bead Studio v. 1.0.0.5) and normalized by Quantile normalization. To determine differentially expressed sets of genes across the three experimental groups, One-way analysis of variance (ANOVA) and LPE testing was used. After following analysis, 15633 genes were selected with the common conditions; (1) P-value of ANOVA $<$ 0.05, (2) |Fold(B/A) $>$ 5 and P-value $<$ 0.05, (3) |Fold(C/A) $>$ 5 and P-value $<$ 0.05. We applied Avadis Prophetic version 3.3 (Strand Genomics, Bangalore, India) software for statistical analyses.

9. SYBR Green real-time polymerase chain reaction

Aliquots of the RNAs used for the microarray experiments were applied to perform validation of the microarray results. Total RNA was extracted from YDOV-21 and six HOSEs (HOSE 18, 19, 21, 40, 41, 59) using the RNeasy Mini kit (Qiagen, Valencia, CA). Next, a total of 2 μg RNA from each sample was reverse transcribed into cDNA by SuperScript ^{TM} III first – strand synthesis system (Invitrogen, Carlsbad, CA) according to the manufacturer's protocol. The expression of candidate gene mRNA was measured by SYBR Green real-time PCR using an ABI 7300 instrument (Applied Biosystems, Forster, CA). The specific primers were listed in Tab. 1. The thermal cycling conditions consisted of a pre-incubation for 2 min at 50^{o}C then denaturation for 10 min at 95^{o}C followed by 40 cycles of denaturation for 15 sec at 95^{o}C and annealing/extension for 1 min at 60^{o}C. The normalization formula was as follows: target amount = $2^{-\Delta\Delta Ct}$, where $\Delta\Delta Ct$ = [Ct (Candidate gene) – Ct (Candidate gene GAPDH)] - [Ct (HOSE186)-Ct (HOSE 186 GAPDH)].

Gene	Forward primer sequence : Reverse primer sequence :
FYN	Forward primer sequence : 5’-AAC TGT GST TGC STC GSG TTG T-3' Reverse primer sequence : 5’-ACT TCA GCG AAA CAC CCC TG-3’
MYBL2	Forward primer sequence : 5’-CCG GAG CAG AGG GAT AGC A-3’ Reverse primer sequence : 5’-CAG TGC GGT TAG GGA AGT GG-3’
SKI	Forward primer sequence : 5’-ACT GGA AGG CGA GSC CAT CT-3’ Reverse primer sequence : 5’-ACA CCG CGT TGA TCT GCT G-3’
RUNX3	Forward primer sequence : 5’-CCT ACC ACC TCT ACT ACG GGA CAT-3' Reverse primer sequence : 5’-CCC ACT GCT GCT GCC G-3’
CDKN2C	Forward primer sequence : 5’-GGA ACC TGC CCT TGC ACT T-3’ Reverse primer sequence : 5’-CGT GTG CTT CAC CAG GAA CTC-3’
CT45A2	Forward primer sequence : 5’-TCC TCT CCC AAA AGC CAA CA-3’ Reverse primer sequence : 5’-ACG CAT CGG AGT TCC TTC AC-3’

Table 1. The sequences of specific primers.

10. 2D electrophoresis

IPG gel strips (Amersham Biosciences Co., Piscataway, NJ) were rehydrated in reswelling solution for 24 h at 20℃. For isoelectric focusing (IEF), 100 μg of each protein sample was applied to the 13 cm immobilized nonlinear pH 3–10 NL strip at 20℃ in five steps: 50, 500, 1,000 V and final step of 60,000 Vh at 8,000 V using Ettan IPGphor II (Amersham Biosciences Co., Piscataway, NJ). After IEF, the strips were equilibrated with buffer (6 M Urea, 75 mM Tris–HCl, 29.3% Glycerol, 2% SDS) and 1% DTT for 15 min as a first step, and with 2.5% iodaacetamide for 15 min as a second step. For SDS gel electrophoresis, a 10% SDS gel was prepared and the equilibrated IPG gel strip was laid on top of the gel and was covered with 0.5% agarose solution. Next, silver staining was applied to the gel. For differential analysis, gels were scanned with an ImageScanner device and analyzed using imageMaster™ 4.01 software (both from Amersham Biosciences). Variations that more than two-fold increasing were taken into consideration.

11. Enzymatic digestion of proteins in-gel

Protein spots in-gel were digested with enzyme as the same technique described by Shevchenko et al. [4] Gel pieces were cleaned with 50% acetonitrile to get rid of SDS, salt, and stain.

After that, Gel pieces were dehydrated to remove solvent, rehydrated with trypsin (8–10 ng/μl) and incubated 8–10 h at 37℃, consecutively. 5 μl of 0.5% trifluoroacetic acid is added to terminate the proteolytic reaction. Tryptic peptides were recovered by combining the aqueous phase from several extractions of gel pieces with 50% aqueous acetonitrile. After concentrating the peptide, C18ZipTips (Millipore) is applied to desalt the mixture. The peptides were eluted in 1–5 μl of acetonitrile. An aliquot of this solution was mixed with an equal volume of a saturated solution of a-cyano-4-hydroxycinnamic acid in 50% aqueous acetonitrile, and 1 μl of the resulting mixture was spotted onto a target plate.

12. MALDI-TOF/PMF analysis and database search

Ettan MALDI-TOF (Amersham Biosciences Co., Piscataway, NJ) Protein analysis was performed. Peptides were evaporated with an N2 laser at 337 nm that utilized a delayed extraction approach. The peptides were accelerated with a 20-Kv injection pulse to measure the time of flight (TOF). The search program ProFound, developed by Rockefeller University, was used for protein identification by peptide mass fingerprinting (PMF) [5]. Spectra were calibrated with trypsin auto-digestion ion peaks (842.510 m/z and 2211.1046 m/z) as internal standards.

III. Results

1. General characteristics (*In vitro* morphology, Growth kinetics, Chemosensitivity test)

In phase contrast microscope, cultured YDOV-21 showed oval, round or polygonal cells in a pavement-like arrangement, piled up without contact inhibition. The cultured cells were easily adherent dish bottom and spread as a sheet of monolayered cell (Fig. 1. a.). Up to date, cultured cell lines have undergone over 30 continuous passages. The cell line was proved to be free from contamination by mycoplasma. Along with electromicroscopic examination, we could find specific electromicroscopic features of CCA ; Cytoplasmic glycogen, short blunted surface villi, and few lipid bodies (Fig. 1. b.).

a. 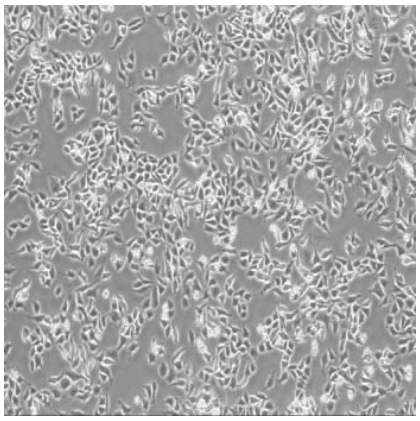 b. 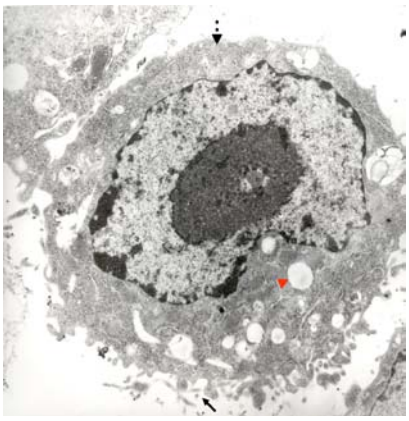

Fig. 1. Microscopic and Electromicroscopic morphology.

a. Phase contrast image, x40 - Cultured cell line showed oval, round or polygonal cells in a pavement-like arrangement, piled up without contact inhibition. Cultured cells easily adherent to dish bottom and spread as a sheet of monolayer cell.

b. Electromicroscopic image, x16000 - Cytoplasmic glycogen (dashed arrow), and short blunted surface villi (arrow), few lipid bodies (arrowhead) that specific features of CCA are noted.

Growth kinetics study of cell lines were performed at specific conditions described in methods section. Analysis of the growth curve of the YDOV-21 cell showed that the population doubling time was 28.7 hours (Fig. 2. a.). FBS concentration did not affect on growth rate of YDOV-21, considerably. The result of chemosensitivity test revealed that the most sensitive chemotherapeutic agent was gemcitabine among the twelve tested drugs. In this experiment, Chemosensitivity of platinum akylating agent such as cisplatin, carboplatin, paclitaxel and docetaxel showed poor potency to YDOV-21 as like to CCA. Details of the inhibition rate and chemosensitivity index are presented (Fig. 2. b.).

a.

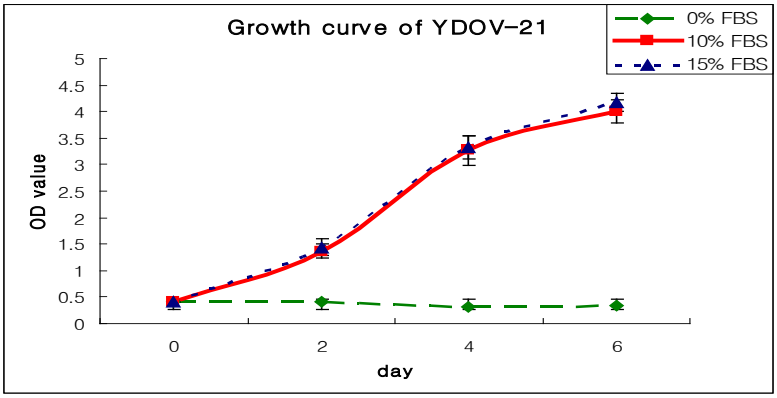

b.

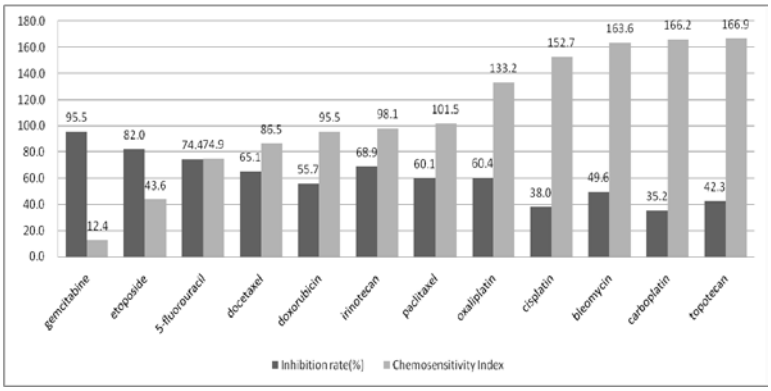

Fig. 2. Growth kinetics and Chemosensitivity test.

a. Growth curves – Under each conditioned FBS concentration and 5% CO2 atmosphere at 37℃, the population doubling time was about 28.7 hours. Concentration of FBS seems to not effect considerably on growth rate.

b. Chemosensitivity test – The most sensitive chemotherapeutic agent was revealed to gemcitabine. YDOV-21 does not show good sensitivity to platinum akylating agent such as cisplatin, carboplatin, paclitaxel and docetaxel. Chemosensitivity index (CI) was calculate as follows: 300 – SUM (% cell suppression 0.2 X－5 X). Black Bar : Inhibition rate (%). Gray Bar : Chemosensitivity index.

2. Tumorigenicity

The YDOV-21 cell line showed highly tumorigenic properties in the nude mice. Average time to tumor mass grew up to 1 cm in diameter took about 18 days and increased up 3 cm in diameter within 30 days after inoculation (Fig. 3. a1, a2.). Visible subcutaneous tumor masses were successfully developed in all the three continuative experiments. Histopathologic findings of xenografted tumor mass were consistent with that of dissected tumor originated from the patient.

In microscopic low power view (X100) of induced tumor masses, multiple small cavities surrounded by atypical epithelium were noted. Fibrovascular stroma was seen among the cavities (Fig. 3. b1.). In high power view (X400), Multiple clusters of cell that have abundant cytoplasm,

polymorphic nucleus, prominent nucleolus and hob-nail cell are found (Fig. 3. b2.). Metastasis to heart, lung and peri-renal lesion were observed in the mice inoculated with YDOV-21 cell line (Fig. 3. c, d, e.).

a1. 

a2. 

b1. 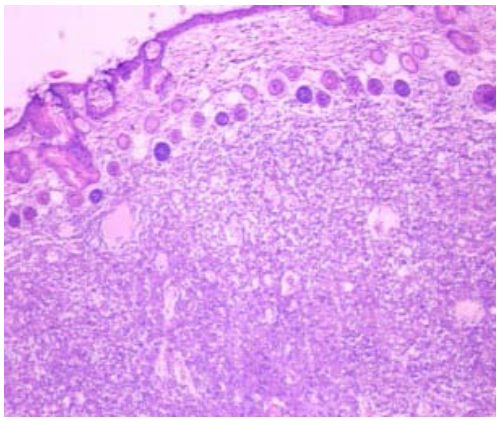

b2. 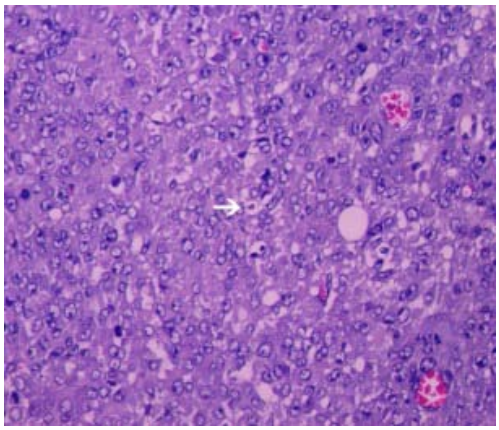

c. 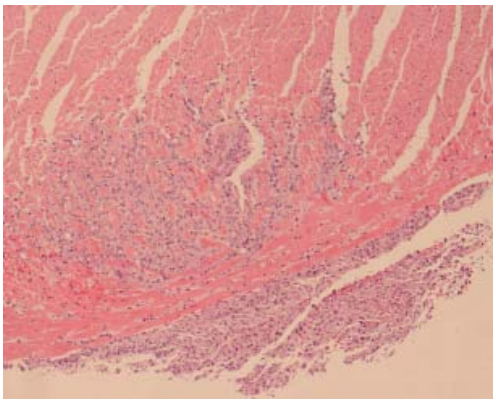

d. 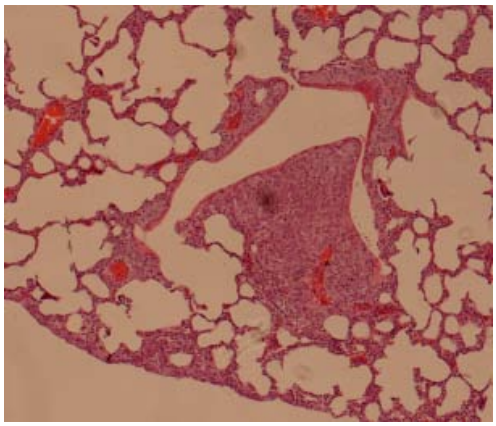

e. 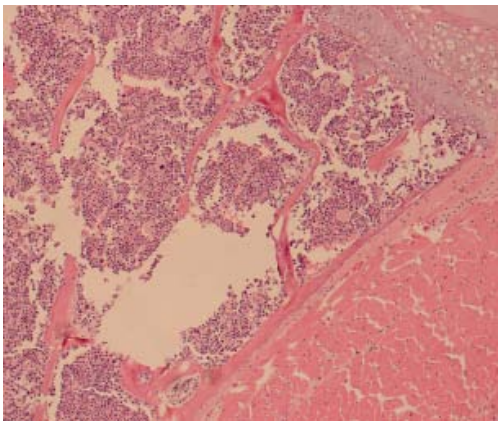

Fig. 3. Tumorigenicity in a nude mouse and microscopic view of induced tumor and metastatic mass.
a1. - 18 days after subcutaneously injection of 2 X 10^3 cells.
a2. - 30 days after subcutaneously injection of 2 X 10^3 cells.
b1. Induced tumor mass, In low power view (X 100) - Multiple small cavities surrounded by atypical epithelium were noted. fibrovascular stroma was seen among the cavities.
b2. Induced tumor mass, In high power view (X 400) - Multiple clusters of cell that have abundant cytoplasm, polymorphic nucleus, prominent nucleolus and hob-nail cell (white arrow) are found.
c. - Metastasis to heart.
d. - Metastasis to lung.
e. - Metastasis to peri-renal lesion.

3. Gene expression profiling

Microarray expression analysis of YDOV-21 and four HOSEs cell lines was done to determine the changes in genes expression patterns. Hierarchical clustering analysis showed that approximately 15,633 genes were differentially expressed (> five-fold, $P < 0.05$). Among the differently expressed genes, Analysis of the data yielded that total 3,983 genes were up-regulated and 4,188 genes were down-regulated in the YDOV-21 cell line. To investigate the association between the differentially expressed genes and functional pathways of ovarian cancer, we grouped some of the genes with remarkable fold change (> five-fold) between the two cell lines according to their function. A partial list of genes that were grouped into the different functional groups is presented in Tables 2.

TargetID	Symbol	Definition	Fold change*	Transcript	Synonym
Oncogene					
ILMN_440	SKI	v-ski sarcoma viral oncogene homolog (avian) (SKI)	**21.00**	NM_003036	SKV
ILMN_9694	MDS1	myelodysplasia syndrome 1 (MDS1)	**18.00**	NM_004991	PRDM3; MDS1-EVI1
ILMN_25662	FYN	FYN oncogene related to SRC, FGR, YES (FYN), transcript variant 2	**9.07**	NM_153047	SLK; SYN; MGC45350
ILMN_8960	RUNX3	runt-related transcription factor 3 (RUNX3), transcript variant 1	**7.46**	NM_001031680	AML2; CBFA3; PEBP2aC
ILMN_8254	AFF1	AF4/FMR2 family, member 1 (AFF1)	**6.61**	NM_005935	AF4; AF-4; PBM1; MLLT2
ILMN_14640	BCL2L14	BCL2-like 14 (apoptosis facilitator) (BCL2L14), transcript variant 4	**6.18**	NM_138723	BCLG
ILMN_3289	LPP	LIM domain containing preferred translocation partner in lipoma (LPP)	**-7.80**	NM_005578	
ILMN_28130	MYC	v-myc myelocytomatosis viral oncogene homolog (avian) (MYC)	**-10.32**	NM_002467	c-Myc
ILMN_10095	LYN	v-yes-1 Yamaguchi sarcoma viral related oncogene homolog (LYN)	**-11.14**	NM_002350	JTK8
Other oncogenesis					
ILMN_5181	VEGF	vascular endothelial growth factor (VEGF), transcript variant 1	**17.37**	NM_001025366	VPF; VEGFA; MGC70609
ILMN_24182	MAGEA12	melanoma antigen family A, 12 (MAGEA12)	**7.00**	NM_005367	MAGE12
ILMN_13838	THSD3	thrombospondin, type I, domain containing 3 (THSD3), transcript variant 1	**6.24**	NM_199296	TAIL1; FLJ32147; MGC119416; DKFZp686E0215
ILMN_23757	ROCK2	Rho-associated, coiled-coil containing protein kinase 2 (ROCK2)	**-5.68**	NM_004850	KIAA0619
ILMN_6129	CTSB	cathepsin B (CTSB), transcript variant 1	**-43.18**	NM_001908	APPS; CPSB
Tumor suppressor					
ILMN_138785	CDKN2	cyclin-dependent kinase inhibitor 2C (p18, inhibits CDK4) (CDKN2C)	**21.78**	NM_078626	p18; INK4C; p18-INK4C
ILMN_20554	CT45A2	cancer/testis antigen CT45-2 (CT45-2), mRNA	**9.44**	NM_152582	
ILMN_28845	BRCA1	breast cancer 1, early onset (BRCA1), transcript variant BRCA1b	**6.43**	NM_007295	IRIS; PSCP; BRCAI; BRCC1; RNF53
ILMN_25102	RBL2	retinoblastoma-like 2 (p130) (RBL2)	**-8.27**	NM_005611	Rb2; P130
ILMN_16446	EIF4EBP2	eukaryotic translation initiation factor 4E binding protein 2 (EIF4EBP2)	**-11.06**	NM_004096	4EBP2
Apoptotic processes					
ILMN_8109	PDCD5	programmed cell death 5 (PDCD5)	**6.24**	NM_004708	TFAR19; MGC9294
ILMN_27679	DNASE1L3	deoxyribonuclease I-like 3 (DNASE1L3)	**5.24**	NM_004944	LSD; DHP2; DNAS1L3
ILMN_11954	ZFR	zinc finger RNA binding protein (ZFR)	**-8.62**	NM_016107	
ILMN_13135	FIS1	fission 1 (mitochondrial outer membrane) homolog (yeast) (FIS1)	**-23.57**	NM_016068	TTC11; CGI-135
ILMN_27899	DNASE2	deoxyribonuclease II, lysosomal (DNASE2)	**-31.91**	NM_001375	DNL; DNL2; DNASE2A

Induction of apoptosis					
ILMN_12148	BCL2L1	BCL2-like 1 (BCL2L1), nuclear gene encoding mitochondrial protein, transcript variant 1	**6.34**	NM_138578	BCLX; BCL2L; Bcl-X; bcl-xL; bcl-xS; BCL-XL/S; DKFZp781P2092
ILMN_14640	BCL2L14	BCL2-like 14 (apoptosis facilitator) (BCL2L14), transcript variant 4	**6.18**	NM_138723	BCLG
ILMN_13385	MAGED2	melanoma antigen family D, 2 (MAGED2), transcript variant 3	**5.49**	NM_201222	11B6; BCG1; HCA10; JCL-1; MAGED; MAGE-D2; MGC8386
ILMN_22318	EBAG9	estrogen receptor binding site associated, antigen, 9 (EBAG9), transcript variant 1	**-6.14**	NM_004215	EB9; PDAF; RCAS1
ILMN_29002	PDCD6IP	programmed cell death 6 interacting protein (PDCD6IP)	**-9.73**	NM_013374	AIP1; Alix; HP95; DRIP4; MGC17003
ILMN_24485	NALP1	NACHT, leucine rich repeat and PYD (pyrin domain) containing 1 (NALP1), transcript variant 5	**-10.37**	NM_001033053	CARD7; DEFCAP; PP1044; KIAA0926; DEFCAP-L/S; DKFZp586O1822
ILMN_3336	BCLAF1	BCL2-associated transcription factor 1 (BCLAF1)	**-22.15**	NM_014739	BTF; KIAA0164; bK211L9.1
ILMN_15265	PDCD6	programmed cell death 6 (PDCD6)	**-56.91**	NM_013232	ALG-2; PEF1B; MGC9123; MGC119050
Inhibition of apoptosis					
ILMN_29093	MYBL2	v-myb myeloblastosis viral oncogene homolog (avian)-like 2 (MYBL2)	**13.02**	NM_002466	BMYB; MGC15600
ILMN_18397	MCL1	myeloid cell leukemia sequence 1 (BCL2-related) (MCL1), transcript variant 1	**11.13**	NM_021960	TM; EAT; MCL1L; MCL1S; MGC1839; MGC104264
ILMN_12148	BCL2L1	BCL2-like 1 (BCL2L1), nuclear gene encoding mitochondrial protein, transcript variant 1	**6.34**	NM_138578	BCLX; BCL2L; Bcl-X; bcl-xL; bcl-xS; BCL-XL/S; DKFZp781P2092
ILMN_9420	BAG3	BCL2-associated athanogene 3 (BAG3)	**-17.56**	NM_004281	BIS; BAG-3; CAIR-1; MGC104307
ILMN_21150	TEGT	testis enhanced gene transcript (BAX inhibitor 1) (TEGT)	**-138.91**	NM_003217	BI-1; TMBIM6
Other apoptosis					
ILMN_4951	PSEN2	presenilin 2 (Alzheimer disease 4) (PSEN2), transcript variant 2	**-8.40**	NM_012486	AD4; PS2; AD3L; STM2
ILMN_18069	TNFSF5IP1	tumor necrosis factor superfamily, member 5-induced protein 1 (TNFSF5IP1)	**-9.87**	NM_020232	PAC2; HCCA3; CLAST3; MDS003; HsT1707; MGC15092
ILMN_1024	PPP1R15A	protein phosphatase 1, regulatory (inhibitor) subunit 15A (PPP1R15A)	**-28.05**	NM_014330	GADD34
ILMN_12802	SCARB2	scavenger receptor class B, member 2 (SCARB2)	**-134.69**	NM_005506	CD36L2; HLGP85; LIMPII; SR-BII
Cell cycle control					
ILMN_6473	AKT2	v-akt murine thymoma viral oncogene homolog 2 (AKT2)	**33.17**	NM_001626	PRKBB; PKBBETA; RAC-BETA
ILMN_440	SKI	v-ski sarcoma viral oncogene homolog (avian) (SKI)	**21.00**	NM_003036	SKV
ILMN_17018	ESR2	estrogen receptor 2 (ER beta) (ESR2)	**10.98**	NM_001437	Erb; ESRB; 5p152; NR3A2; ER-BETA; ESR-BETA
ILMN_25662	FYN	FYN oncogene related to SRC, FGR, YES (FYN), transcript variant 2	**9.07**	NM_153047	SLK; SYN; MGC45350
ILMN_897	BCCIP	BRCA2 and CDKN1A interacting protein (BCCIP), transcript variant B	**8.68**	NM_078468	TOK-1
ILMN_18543	BRMS1	breast cancer metastasis suppressor 1 (BRMS1), transcript variant 3	**-5.85**	NM_001024958	DKFZp564A063

ILMN_25102	RBL2	retinoblastoma-like 2 (p130) (RBL2)	**-8.27**	NM_005611	Rb2; P130
Cell proliferation					
ILMN_29093	MYBL2	v-myb myeloblastosis viral oncogene homolog (avian)-like 2 (MYBL2)	**13.02**	NM_002466	BMYB; MGC15600
DNA replication					
ILMN_4431	ORC2L	origin recognition complex, subunit 2-like (yeast) (ORC2L)	**15.89**	NM_006190	ORC2
ILMN_19993	CSPG6	chondroitin sulfate proteoglycan 6 (bamacan) (CSPG6)	**7.65**	NM_005445	BAM; BMH; HCAP; SMC3; SMC3L1
ILMN_12445	PSF1	DNA replication complex GINS protein PSF1 (PSF1)	**5.94**	NM_021067	KIAA0186; RP4-691N24.2
ILMN_20255	GMNN	geminin, DNA replication inhibitor (GMNN)	**-5.76**	NM_015895	Gem; RP3-369A17.3
ILMN_16870	RFC4	replication factor C (activator 1) 4, 37kDa (RFC4), transcript variant 1	**-6.60**	NM_002916	A1; RFC37; MGC27291
ILMN_26088	RPA1	replication protein A1, 70kDa (RPA1)	**-8.93**	NM_002945	HSSB; RF-A; RP-A; REPA1; RPA70
ILMN_20681	POLD2	polymerase (DNA directed), delta 2, regulatory subunit 50kDa (POLD2)	**-50.37**	NM_006230	

*log fold change YDOV-21 vs HOSEs

Table 2. Selected up and down regulated genes are listed. Approximately 15,633 genes were differentially expressed (> five-fold, $P < 0.05$). Among the differently expressed genes, 3,983 genes were up-regulated and 4,188 genes were down-regulated in the YDOV-21 cell line.

4. SYBR Green real-time PCR analysis of selected gene products

We chose six upregulated genes: FYN, MYBL2, SKI, RUNX3, CDKN2C and CT45A2 to validate the altered expression observed by the cDNA microarray. Expression of those genes were analyzed the along with SYBR Green real-time RT-PCR. All candidate genes of YDOV-21 were highly expressed more than two-fold than those of six HOSEs (Fig. 4.). In general, SYBR Green real-time RT-PCR results were consistent with the expression patterns of the microarray data.

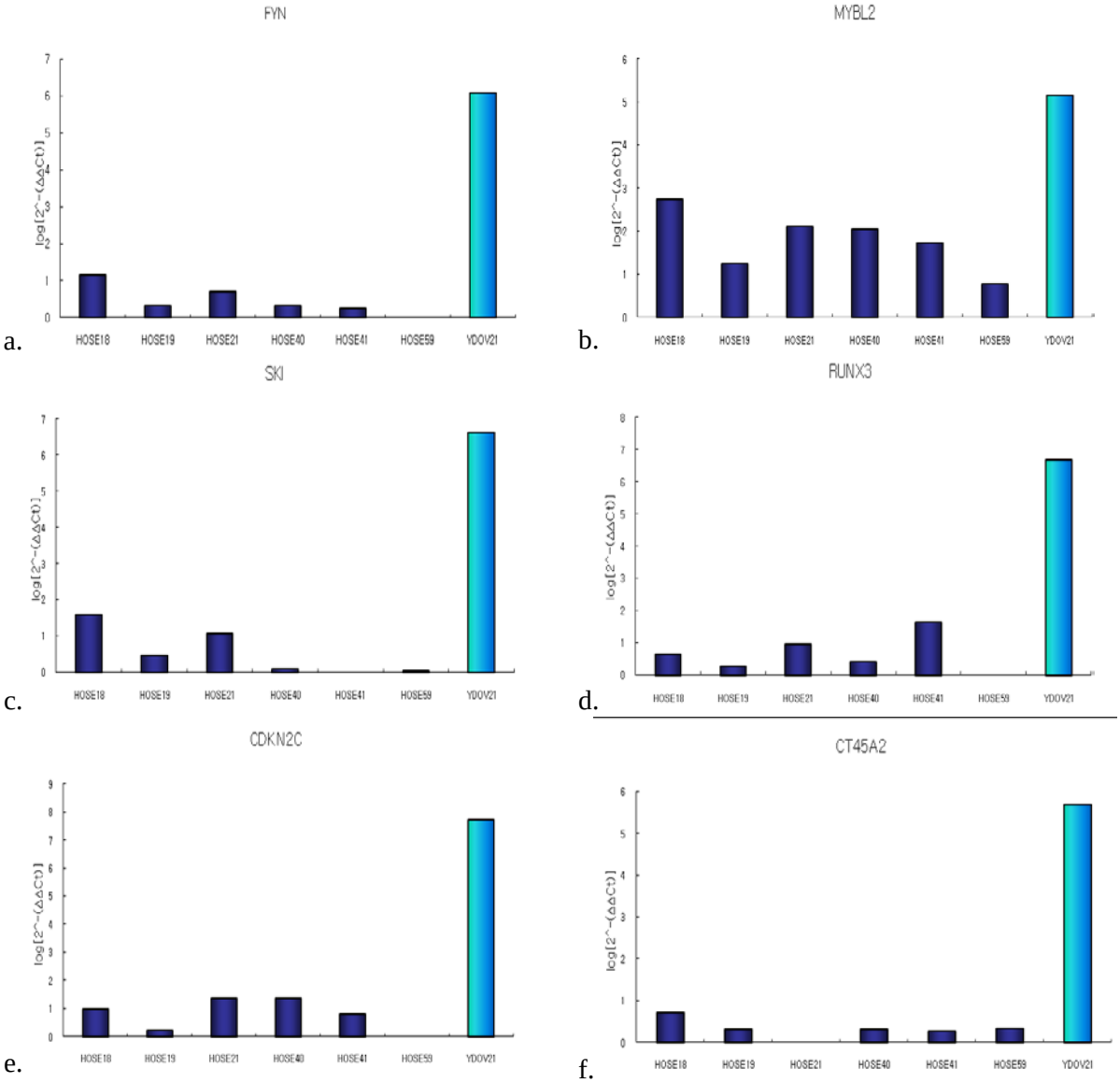

Fig. 4. Validation of cDNA microarray was performed using SYBR Green real-time PCR. Fold change of four genes coding a. FYN, b. MYBL2, c. SKI, d. RUNX3, e. CDKN2C and CT45A2 were compared between YDOV-21 and six HOSEs. All the candidate genes of YDOV-21 were highly expressed more than two-fold than these of six HOSEs.

5. Proteomic analysis

Differently expressed proteins in the YDOV-21 as compared to HOSEs were analyzed by

MALDI-TOF/PMF for protein identification. The horizontal and vertical dimensions of the 2-DE protein content map are plotted in terms of the selected pI range and protein intact Mw, respectively. In the current study, 31 up-regulated proteins in the YDOV-21 were observed (Fig. 5.). The proteins that have been identified by MALDI-TOF/PMF are listed (Table 3).

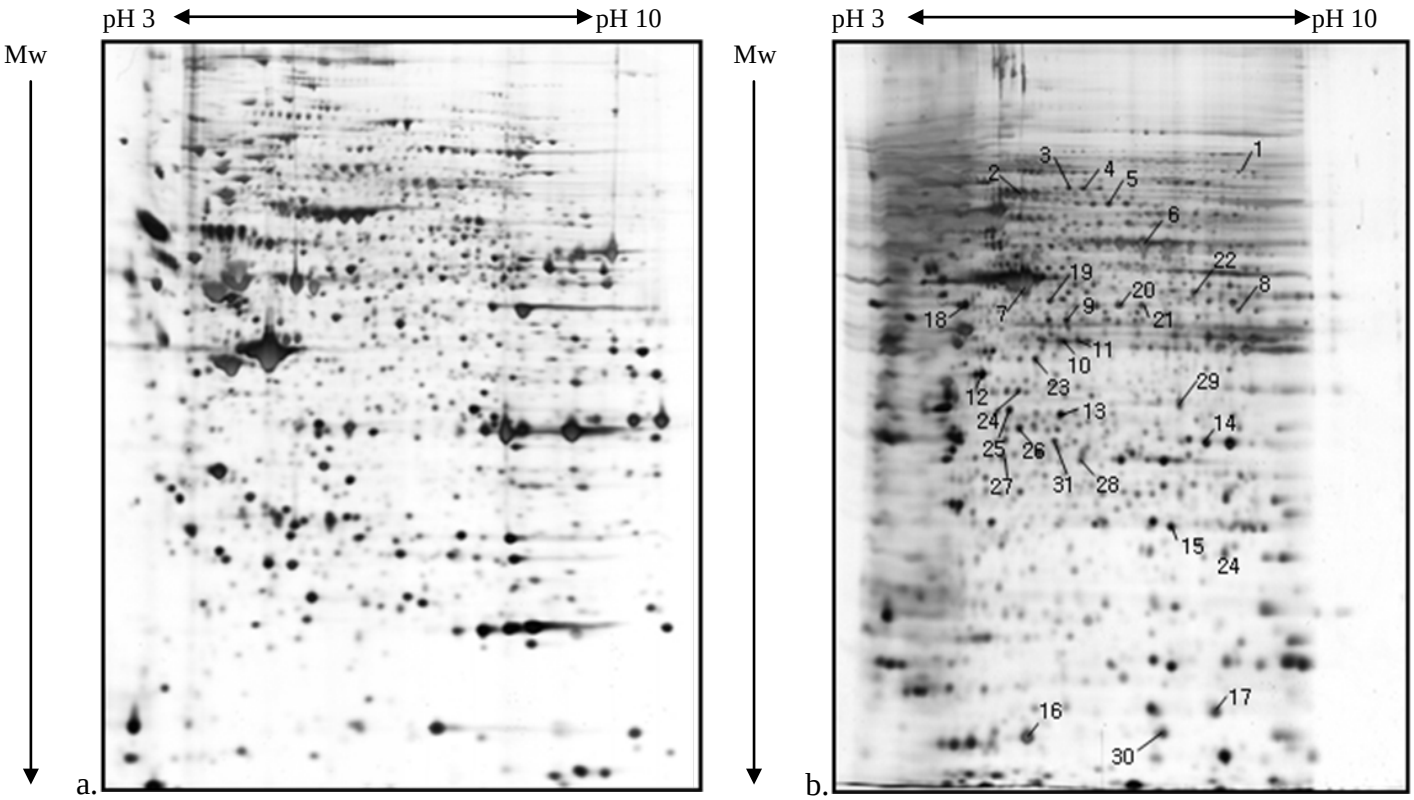

Fig. 5. Proteomic comparison between a. HOSEs and b. YDOV-21 cell line using 2-DE and MALDI-TOF. 100 ug of total protein extract was loaded on pH3-10NL strip, followed by a 10% SDS-PAGE and silver staining lines indicate identified protein spots significantly altered in YDOV-21 as compared to HOSEs. Corresponding identifications are listed in Table. 3.

Spot No.	Identification	% Coverage	pI	Mw (kDa)
Up-regulation (more than two-fold).				
1	Far upsteram element-binding protein	9	7.2	67.7
2	chaperonin	18	5.7	61.2
3	T-complex protein 1 isoform a	23	5.8	60.8
4	T-complex protein 1 isoform a	14	5.8	60.8
5	Protein disulfide-isomerase A3 recursor	19	6.0	57.1
6	Enolase 1	31	7.0	47.4
7	ACTB protein	53	5.6	40.5
8	Sub2.3	24	6.2	32.1
9	Ischemia/reperfusion inducible protein transcript variant 1	14	9.0	28.6
10	Keratin 1	19	8.3	66.2
11	Ribosomal protein, large, P0	34	5.4	34.4
12	Chain A , The effect of metal binding on the structure of annexin V And implications for membrane binding	40	4.9	35.8
13	PHB	20	5.6	29.8
14	Phosphoglycerate mutase 1	51	6.7	28.9
15	Chain B, Crystal structure of A cytokinereceptor complex	20	5.5	21.1
16	C-type lectin domain family 4, member C isoform 1	20	6.6	25.5
17	Ribosomal protein S12	32	6.8	14.9
18	Laminin-binding protein	39	4.8	31.8
19	Testis serine protease 3	17	5.5	42.8
20, 21	Unnamed protein product	30	7.9	14.6
22	Capping protein (actin filament), gelsolin-like	13	6.5	39.0
23	DEAD-box protein	16	9.1	73.3
24	IKK-related kinase epsilon	13	8.3	81.1
25	Nuclear chloride channel	21	5.0	27.25
27	Rho GDP dissociation inhibitor (GDI) alpha	32	5.1	23.4
28	Keratin 1	12	8.3	66.2
29	Purine nucleoside phosphorylase	28	5.9	32.5
30	Otoferlin isoform d	10	5.9	141.3
31	STIM2 protein	11	7.5	63.0

Table 3. Differentially expressed proteins of YDOV-21 in comparison to HOSEs. 31 up-regulated proteins were identified.

IV. Discussion

Throughout this research, we establish a novel CCA cell line and investigate its biological characteristics. CCA has been classified as subgroup of epithelial ovarian carcinoma and well known for unique clinical features. Therefore, well characterization of YDOV-21 might be helpful to understand CCA.

The cultured cells maintained consistent morphology from primary culture to the following subculture passage. YDOV-21 appears to be a permanent cell line: YDOV-21 cell have grown continuously undergoing over 30 passages; growth continues even after recovery from cryopreservation. Cultured cell proved to be highly tumorigenic when injected into nude mice, and the xenotransplanted tumor of YDOV-21 had similar microscopic morphology to the original tumor from which the cell line was derived. Although it is widely accepted that In-vitro chemosensitivity results are different from those of *In vivo*, the significance of our investigation is to provide basis for studying inter-relation between chemosensitivity and proteomic characteristic, which might help make drug selection guidance in the future [6]. As proven by the growth kinetic and xenograft experiments, YDOV-21 shows rapid growth and early metastatic capacity in comparison to previously reported CCA cell line [7-9]. We find a possibility of the cell line as source of cancer stem cell research [10]. Because YDOV-21 has several biologic properties as a cancer stem cell ; Ability to induce cancer mass with low numbers cell count, high success rate of tumor mass induction and early metastasis to other organ.

Distinctive clinical features of CCA are thought to be originated from unique genetic problems and effecter proteins. Therefore, improved understanding of the etiology of the disease and of the pathologic and molecular characteristics of CCA would allow for more strategic and selective treatment regimen for individual patients. Recent studies based on comprehensive gene expression profiling have shown that CCA can be distinguished from other poor prognosis ovarian carcinomas based on their gene expression signature [11]. And CCA has unique cell cycle regulatory pattern among the ovarian adenocarcinoma [12]. Among the up-regulated gene of YDOV-21, The RUNX3 transcription factor is a downstream effecter of the transforming growth factor-beta (TGF-beta) signaling pathway, and has a critical role in the regulation of cell proliferation and cell death by apoptosis, and in

angiogenesis, cell adhesion and invasion [13]. RUNX3 was thought to be related to various malignancies such as gastric cancer, multiple solid tumors, lung cancer and others [14-16]. Recent study has revealed that RUNX3 has a role in cell proliferation and viability in ovarian cancer [17]. In this study, Immunofluorescent staining confirmed upregulation of cytoplasmic RUNX3 in ovarian cancer cell lines and tissues. On another study, the methylation of the RUNX3 gene promoter region plays a critical role in the regulation of RUNX3 repression, and that it is significantly correlated with RUNX3 mRNA expression in ovarian cancer tissues [18]. An increase of the RUNX3 of YDOV-21 was consistent with that of previous literatures. We believe that additional research is needed on how Epigenetic mechanism of RUNX3 act on the YDOV-12.

As reported in many previous researches, most case of ovarian cancer was already progressed when it was diagnosed [19]. This is the reason for emphasizing the importance of screening test. Until now, there is no clinically applicable biomarker for CCA. If there is reliable biomarker for detection of early stage malignancy including CCA, this eventually leads to the development of new type-specific diagnostic and/or therapeutic strategies that might significantly improve survival. 2-DE techniques that use labeled proteins make it possible to detect expression differences, including proteins expressed in low amounts, with good accuracy [20]. Considering this advantages, we compared the protein profiles of YDOV-21 with that of the eight HOSEs and indentified 31 up-regulated proteins. According to the survey of previous researches, there is not much for the proteomic study of CCA. Morita et al published the only study on proteomes of CCA cell lines (OVISE, OVTOKO), but they compared the protein profiles of CCA and those of mucinous adenocarcinoma cell [21]. As we know, current study is the first that compared the proteomes of the CCA cell line and the normal ovarian cell lines.

Along with the YDOV-21 cell line, we can make a step forward to understand the CCA. But there are many problems to solve; especially the correlations between *In vitro* genomic / proteomic characterization and the clinical relevant course such as prognosis and treatment option. One limitation of the current study is that comparative genomic and proteomic studies enrolled only two cell lines (YDOV-21 and HOSEs). Although we suggested several up-regulated proteins as potential

candidate of biomarker, comparative study recruiting more CCA and normal cells are needed to give more confidence and specificity.

V. Conclusion.

Through this research, we established a novel CCA cell line named YDOV-21 and conducted research on biological characteristics of it. For all we know, this study is the first that compare the genomic & proteomic profiles of CCA to that of the normal HOSE cells. Although we did not enrolled many CCA cells in the experiment, current study results play a basic role in molecular understanding of YDOV-21. Further investigations are thought to be needed about correlation between the clinical characteristics and identified the genomic, proteomic profiles of YDOV-21.

1. Crozier MA, Copeland LJ, Silva EG, Gershenson DM, Stringer CA. Clear cell carcinoma of the ovary: a study of 59 cases. Gynecol Oncol 1989 Nov;35(2):199-203.
2. Sugiyama T, Kamura T, Kigawa J, Terakawa N, Kikuchi Y, Kita T, et al. Clinical characteristics of clear cell carcinoma of the ovary: a distinct histologic type with poor prognosis and resistance to platinum-based chemotherapy. Cancer 2000 Jun 1;88(11):2584-9.
3. Fehrmann RS, Li XY, van der Zee AG, de Jong S, Te Meerman GJ, de Vries EG, et al. Profiling studies in ovarian cancer: a review. Oncologist 2007 Aug;12(8):960-6.
4. Shevchenko A, Wilm M, Vorm O, Mann M. Mass spectrometric sequencing of proteins silver-stained polyacrylamide gels. Anal Chem 1996 Mar 1;68(5):850-8.
5. Zhang W, Chait BT. ProFound: An Expert System for Protein Identification Using Mass Spectrometric Peptide Mapping Information. analytical chemistry 2000 May 4, 2000;72(11):2482-9.
6. Jain KK. Role of oncoproteomics in the personalized management of cancer. Expert Rev Proteomics 2004 Jun;1(1):49-55.
7. Sasa H, Ishii K, Hirata J, Kikuchi Y, Nagata I, Kawai T, et al. [Establishment and characterization of a CA125-producing human ovarian clear cell carcinoma cell line]. Hum Cell 1993 Dec;6(4):279-86.
8. Wong WS, Wong YF, Ng YT, Huang PD, Chew EC, Ho TH, et al. Establishment and characterization of a new human cell line derived from ovarian clear cell carcinoma. Gynecol Oncol 1990 Jul;38(1):37-45.
9. Fushiki H, Hidaka T, Fujimura M, Yasoshima K, Yamakawa Y, Izumi R. Characterization of a newly established human tumor cell line (TEN) from a patient with clear cell carcinoma of the uterine body and its sensitivity to anti-cancer agents. Hum Cell 1997 Sep;10(3):199-208.
10. Tan BT, Park CY, Ailles LE, Weissman IL. The cancer stem cell hypothesis: a work in progress. Lab Invest 2006 Dec;86(12):1203-7.
11. Schwartz DR, Kardia SL, Shedden KA, Kuick R, Michailidis G, Taylor JM, et al. Gene expression in ovarian cancer reflects both morphology and biological behavior, distinguishing clear cell from other poor-prognosis ovarian carcinomas. Cancer Res 2002 Aug 15;62(16):4722-9.
12. Shimizu M, Nikaido T, Toki T, Shiozawa T, Fujii S. Clear cell carcinoma has an expression pattern of cell cycle regulatory molecules that is unique among ovarian adenocarcinomas. Cancer 1999 Feb 1;85(3):669-77.
13. Subramaniam MM, Chan JY, Yeoh KG, Quek T, Ito K, Salto-Tellez M. Molecular pathology of RUNX3 in human carcinogenesis. Biochim Biophys Acta 2009 Dec;1796(2):315-31.
14. Gao N, Chen WC, Cen JN. [Relationship between Runx3 gene expression and its DNA methylation in gastric cancer]. Zhonghua Zhong Liu Za Zhi 2008 May;30(5):361-4.
15. Araki K, Osaki M, Nagahama Y, Hiramatsu T, Nakamura H, Ohgi S, et al. Expression of RUNX3 protein in human lung adenocarcinoma: implications for tumor progression and prognosis. Cancer Sci 2005 Apr;96(4):227-31.
16. Hsu PI, Hsieh HL, Lee J, Lin LF, Chen HC, Lu PJ, et al. Loss of RUNX3 expression correlates with differentiation, nodal metastasis, and poor prognosis of gastric cancer. Ann Surg Oncol 2009 Jun;16(6):1686-94.
17. Nevadunsky NS, Barbieri JS, Kwong J, Merritt MA, Welch WR, Berkowitz RS, et al. RUNX3 protein is overexpressed in human epithelial ovarian cancer. Gynecol Oncol 2009 Feb;112(2):325-30.
18. Zhang S, Wei L, Zhang A, Zhang L, Yu H. RUNX3 gene methylation in epithelial ovarian cancer tissues and ovarian cancer cell lines. OMICS 2009 Aug;13(4):307-11.
19. Roett MA, Evans P. Ovarian cancer: an overview. Am Fam Physician 2009 Sep 15;80(6):609-16.
20. Yan JX, Devenish AT, Wait R, Stone T, Lewis S, Fowler S. Fluorescence two-

dimensional difference gel electrophoresis and mass spectrometry based proteomic analysis of Escherichia coli. Proteomics 2002 Dec;2(12):1682-98.
21. Morita A, Miyagi E, Yasumitsu H, Kawasaki H, Hirano H, Hirahara F. Proteomic search for potential diagnostic markers and therapeutic targets for ovarian clear cell adenocarcinoma. Proteomics 2006 Nov;6(21):5880-90.

ABSTRACT(IN KOREAN)

투명세포 선암종 세포주(YDOV-21)의 확립과 Genomic, Proteomic 연구를 포함한 세포주의 특성화 연구

<지도교수 김 재 훈>

연세대학교 대학원 의학과

채 용 현

새로운 투명세포 선암종(CCA) 세포주의 확립은 CCA의 생물학적 특성과 암화 과정에 대한 연구를 촉진하는 기초가 된다. 이번에 YDOV-21이라 명명된 새로운 CCA 세포주는 FIGO 병기 IIIb로 진단된 53세 대한민국 여성으로부터 유래되었으며, 오랫동안 성공적으로 계대 배양 되었다. YDOV-21의 특성화 연구를 위하여 *In vitro* 상태에서의 형태와 모양, 성장 곡선, 종양형성능력에 대한 연구를 진행하였다. 또한 CCA의 독특한 임상적 특성에 대한 이해를 넓히고자 이 세포주의 genomic, proteomic 특성에 대한 연구도 함께 하였다. 연구 결과 YDOV-21 세포주는 위상차 현미경 소견상 세포들은 타원형과 방추형 혹은 다각형의 형태를 가지고 있었으며 세포간의 접촉에 의한 억제현상 없이 단층으로 성장하는 모습을 관찰할 수 있었다. 세포주의 성장배가 시간은 약 28.7시간으로 매우 빠른 성장 속도를 보여주으며, 12가지 항암화학약물에 대한 감수성 조사에서는 gemcitabine에 대해서 가장 높은 감수성을 보였다. 또한 쥐를 이용한 종양형성능력 실험에서는 높은 종양 능력을 나타내었으며, 암 세포의 타 장기로의 원격 전이도 비교적 이른 시기에 관찰할 수 있었다. 4개의 HOSEs 세포주과 비교한 Microarray 실험에서는 3,983개의 과발현된 유전자와 4,188개의 과소발현된 유전자를 관찰할 수 있었다 (> five-fold, $P < 0.05$). 이 결과는 SYBR Green real-time RT-PCR 방법을 이용한 Validation 실험에서도 일치된 결과를 확인할 수 있었다. HOSEs 세포주를 대조군으로 사용한 2-DE 실험에서는 31개의 2배 이상 과발현된 점들이 발견되었다.

핵심되는 말 : 세포주 투명세포 선암종, Microarray, proteomic profile, 2D